Optical Properties and Aging of Light Absorbing Secondary Organic Aerosol

Jiumeng Liu[1], Peng Lin[2], Alexander Laskin[2], Julia Laskin[3], Shawn M. Kathmann[3], Matthew Wise[4], Ryan Caylor[4], Felisha Imholt[4], Vanessa Selimovic[4‡], John E. Shilling[1,*]

[1] Atmospheric Sciences and Global Change Division, Pacific Northwest National Laboratory Richland, WA, USA.

[2] Environmental Molecular Sciences Laboratory, Pacific Northwest National Laboratory, Richland, WA, USA.

[3] Physical Sciences Division, Pacific Northwest National Laboratory, Richland, WA, USA.

[4] Math and Science Department, Concordia University, Portland, OR, USA.

[‡]Now at Department of Chemistry, University of Montana, Missoula, Montana 59812, USA

*Correspondence to: John E. Shilling (john.shilling@pnnl.gov)

Keywords: Secondary Organic Aerosol, Brown Carbon, Light Absorption

Abstract

The light-absorbing organic aerosol (OA), commonly referred to as "brown carbon (BrC)", has attracted considerable attention in recent years because of its potential to affect atmospheric radiation balance, especially in the ultraviolet region and thus impact photochemical processes. A growing amount of data has indicated that BrC is prevalent in the atmosphere, which has motivated numerous laboratory and field studies; however, our understanding of the relationship between the chemical composition and optical properties of BrC remains limited. We conducted chamber experiments to investigate the effect of various VOC precursors, NO_x concentrations, photolysis time and relative humidity (RH) on the light absorption of selected secondary organic aerosols (SOA). Light absorption of chamber generated SOA samples, especially aromatic SOA, was found to increase with NO_x concentration, at moderate RH, and for the shortest photolysis aging times. The highest mass absorption coefficients (MAC) value is observed from toluene SOA products formed under high NO_x conditions at moderate RH, in which nitro-aromatics were previously identified as the major light absorbing compounds. BrC light absorption is observed to decrease with photolysis time, correlated with a decline of the organonitrate fraction of SOA. SOA formed from mixtures of aromatics and isoprene absorb less visible and UV light than SOA formed from aromatic precursors alone on a mass basis. However, the mixed-SOA absorption was underestimated when optical properties were predicted using a two-product SOA formation model, as done in many current climate models. Further investigation, including analysis on detailed mechanisms, are required to explain the discrepancy.

1. Introduction

Climate forcing by various atmospheric components has been intensely investigated over the last few decades but significant uncertainties still exist (IPCC, 2013). One of the largest uncertainties comes from the role of carbonaceous aerosols, including black carbon (BC) and organic carbon (OC). Black carbon is formally defined as an ideally light-absorbing substance composed of carbon (Petzold et al., 2013) with strong absorption across a wide spectrum of visible wavelengths, which is caused by a significant, wavelength-independent imaginary part k (i.e., ~0.79 (Bond et al., 2013)) of the refractive index. BC has long been known as the strongest light-absorbing aerosol in the visible wavelengths (e.g., Bond et al., 2013). On the other hand, OC has been treated as a scattering species, and only a few recent global modeling studies have focused on the radiative forcing by absorbing OC (Lin et al., 2014a; Feng et al., 2013;Chung et al., 2012). Light absorbing OA are collectively called brown carbon (BrC) (Laskin et al., 2015;Moise et al., 2015;Andreae and Gelencsér, 2006). In contrast to BC, the imaginary refractive index of BrC has stronger wavelength dependence (λ^{-2}–λ^{-6}) that increases towards shorter visible and ultraviolet (UV) wavelengths. This broad absorption band in the blue/violet region of the spectrum gives BrC its eponymous yellow or brown color (Alexander et al., 2008;Andreae and Gelencsér, 2006;Lukács et al., 2007). BrC has been widely observed in many environments, including urban environments largely impacted by anthropogenic emissions(Zhang et al., 2013;Du et al., 2014), biomass burning plumes(Lack et al., 2013;Lack et al., 2012;Forrister et al., 2015), over the ocean(Bikkina and Sarin, 2013), rainwater(Kieber et al., 2006) and in the troposphere(Liu et al., 2014;Alexander et al., 2008).

A variety of studies have investigated sources of BrC in both the laboratory and in the field. Incomplete and smoldering combustion of hydrocarbons, especially those associated with biomass burning, is known to directly produce particulate BrC (Hoffer et al., 2006;Hecobian et al., 2010;Lack et al., 2013;Desyaterik et al., 2013;Chakrabarty et al., 2010;Kirchstetter and Thatcher, 2012;Mohr et al., 2013). There is also evidence based on ambient studies of a secondary BrC source (Duarte et al., 2005) and laboratory studies show formation of chromophores (components of molecules that absorb light) through a variety of mechanisms, including photooxidation of aromatics (Lambe et al., 2013;Liu et al., 2015b), ozonolysis of terpenes subsequently aged in the presence of ammonium ions and humidity (Bones et al., 2010;Nguyen et al., 2013;Laskin et al., 2014;Updyke et al., 2012), and a variety of additional aqueous phase reactions, such as lignin (Hoffer et al., 2006) and isoprene oxidation (Limbeck et al., 2003), reactions of carbonyls (e.g., glyoxal, methyglyoxal) in acidic solutions(Sareen et al., 2010), with amino acids (De Haan et al., 2009), amines (De Haan et al., 2009;Powelson et al., 2014;Zarzana et al., 2012), or ammonium salts (Sareen et al., 2010;Lin et al., 2015a;Galloway et al., 2009;Kampf et al., 2012;Shapiro et al., 2009). Among those studies, it is suggested that the chemical and optical properties of laboratory generated SOA might be influenced by a variety of factors, including the composition of the volatile organic carbon (VOC) precursor, oxidation chemistry, relative humidity (RH), and potentially "aging" at longer time scales (i.e., in-particle reactions and photobleaching). Particularly, SOA aged in the presence of dissolved ammonium has been shown to produce BrC efficiently, which may contribute to aerosol optical density in regions with elevated concentrations of ammonium salts (i.e., Updyke et al., 2012).

This study focuses on measuring light absorption by laboratory-generated SOA that simulate both urban and remote environments. Four VOCs representative of biogenic and anthropogenic emission are chosen as SOA precursors in this study. Biogenic VOCs selected include isoprene and α-pinene, of which isoprene is the most abundant biogenic non-methane hydrocarbon emitted into the atmosphere (Guenther et al., 2006), while α-pinene accounts for approximately 40% of global monoterpene ($C_{10}H_{16}$) emissions (Guenther et al., 2012). For anthropogenic VOCs, we selected trimethylbenzene (TMB) and toluene, the photooxidation of which in the presence of NO_x is a major source of anthropogenic SOA (Ng et al., 2007;Kleindienst et al., 2004;Henze et al., 2008). Four different types of experiments were conducted to investigate the effects of (1) NO_x levels, (2) VOC precursors, (3) photolysis time, and (4) RH on SOA light absorption. We compare the light absorption of formed SOA by ultraviolet/visible (UV/Vis) absorption measured from aerosol samples extracted in water and methanol.

2. Experimental methods

Experiments were performed in the indoor 10.6 m^3 Teflon chamber at the Pacific Northwest National Laboratory (PNNL) operating in batch mode where a discrete quantity of a VOC is introduced into the chamber and allowed to react with the gas-phase oxidants (Liu et al., 2012). The Teflon chamber was flushed continuously with dry purified air until particle concentrations were less than 5 cm^{-3} prior to all experiments. For each experiment, a measured amount of VOC was injected into a glass bulb with a syringe, evaporated with gentle heating, and transferred to the chamber in a flow of purified air. After the VOC injection, 0.5 mL of H_2O_2 solution (Sigma-Aldrich, 50 wt% in H_2O) was injected into the chamber in the same manner. Humidity was controlled by passing pure air at a variable flow rate

through pure water (18.2 MΩ cm, <5ppbv TOC) with a HEPA filter downstream of the bubbler to remove any contaminant particles. In experiments in which NO_x were present, NO was injected from a gas cylinder containing a known NO concentration (500 ppm, Matheson Tri-Gas®) with flows regulated by mass flow controllers. After all components were injected and well-mixed in the chamber, UV lights were turned on to initiate photooxidation. The UV flux in the chamber, averaged J_{NO2}=0.16 min^{-1}, was measured continuously by a radiometer that is calibrated to an equivalent photolysis rate of NO_2 and suspended in the center of the chamber. Measurements of J_{NO2} using the photostationary state method were in agreement with the radiometer measurements (Leighton, 1961).

During the experiments, a suite of online instruments were used to characterize the gas- and particle-phase composition. The mixing ratios of the hydrocarbons were continuously monitored with an Ionicon proton-transfer-reaction mass spectrometry (PTR-MS). The mass loading of the aerosol particles was measured using an Aerodyne high-resolution time of flight mass spectrometer (HR-ToF-AMS) (DeCarlo et al., 2006), while the number and volume concentrations were measured with a TSI scanning mobility particle sizer (SMPS). An $NO/NO_2/NO_x$ analyzer (Thermo Environmental Instruments model 42c) was used to measure the concentration of NO and NO_x. A UV absorption O_3 analyzer (Thermo Environmental Instruments model 49C) allowed for the measurement of O_3 concentration.

SOA samples were collected on filters to measure their light absorption. Photooxidation products were collected onto PTFE filters (Pall Life Sciences, 47 mm, 1 μm pore size) at a flow rate of 9 L min^{-1} for a

collection period of 60-120 minutes. Typically at least 20 μg of organic mass is required for accurate measurement of light absorption. As described in previous studies (Hecobian et al., 2010;Zhang et al., 2011), filters were extracted in high purity water (> 18.2 MΩ cm), filtered through a 25mm diameter 0.45 μm pore syringe filter (Fisher Scientific, Fisherbrand™ Syringe Filters) and transferred into a long-path (100 cm pathlength) UV-Visible spectrometer (Ocean Optics) to determine the light-absorption spectra. After water extraction, filters were also sonicated in methanol (VWR International, A.C.S. Grade) to extract non-water soluble mass (Liu et al., 2013;Liu et al., 2015a). Total absorption due to BrC (Abs(λ)) is determined as the sum of water-soluble and methanol-extracted absorption from the sequential extraction processes. An extraction efficiency test was performed with 6 filters, in which filters were cut in halves, one half extracted with methanol only and the other half processed with the sequential extraction. Results show that the sum of light absorption from the sequential extraction is comparable to methanol extraction alone, with a slope within 8% of 1 (Figure S1). Studies have shown that the extraction efficiency of organic mass is >90% using methanol as the solvent (Chen and Bond, 2010;Updyke et al., 2012). Thus, it is reasonable to assume that total light absorption determined from the sequential extraction procedure closely approximates the "true" optical properties of the SOA samples. The limit of detection (LOD) was 0.081 Mm^{-1} in the 300-700 nm wavelength range with an estimated uncertainty of 21%. The mass absorption coefficient (MAC) was then estimated using equation 1:

$$MAC(\lambda) = \frac{Abs(\lambda)}{OM} \quad (1)$$

in which Abs(λ) is the light absorption from filter-collected aerosol samples at a wavelength λ, and OM is the SOA mass concentrations on the filter estimated from AMS measurements and the sampled air

volume. Wall-loss corrections were not applied to either measured SOA mass concentrations or light absorption determined from filter-collected aerosol samples for consistency. Based on lowest SOA mass concentrations during all experiments, the LOD of the MAC is estimated as 0.004 m^2 g^{-1}.

2.1 Description of the SOA two-product model

Ambient studies have shown that SOA produced from urban emissions in isoprene-rich environments tend to have much lower BrC absorption compared to that in anthropogenic emission dominant environments (Zhang et al., 2011). In our study, two mixed precursor experiments were conducted to investigate the changes in aromatic BrC due to addition of isoprene reaction products. We employ a two-product model to describe the partitioning of organic mass between aromatic- and isoprene-derived SOA (Pankow, 1994;Odum et al., 1996). SOA yield parameters for pure compounds are determined by fitting real-time batch mode data as described in the literature (Presto and Donahue, 2006). In the mixed precursor experiments, the PTR-MS data is used to determine the amount of each precursor reacted during the filter collection periods. Then, the pure compound yield parameterizations are used to calculate the relative fractions of the isoprene- and aromatic-derived SOA collected on the filter. The calculation assumes that all SOA components are mutually miscible and reproduced the measured SOA mass with the difference less than 10% (Table S2). These fractions are then used along with the optical properties of the single-precursor SOA to predict the optical properties of the mixed aerosol.

3. Results and Discussion

3.1 Effects of VOC types and NO_x levels

163 The wavelength-dependent MAC values for SOA derived from four selected precursor VOCs are
164 plotted in Figure 1. In general, the shapes of the spectra are characteristic of typical atmospheric BrC
165 materials, with relatively higher absorption in the UV range (i.e., Hecobian et al., 2010;Chen and Bond,
166 2010). Figure 2 shows a comparison of the MAC at 365 nm among four different SOA samples
167 (isoprene, α-pinene, TMB and toluene) produced under NO_x-free and high-NO_x conditions.
168
169 The MAC values of isoprene SOA are close to the LOD in the 300-700 nm wavelength range and there
170 is no significant difference in the UV-Vis spectra of isoprene SOA formed under NO_x-free and high-
171 NO_x conditions. Quantum mechanical calculations suggest that electrons must be delocalized over the
172 equivalent of 7-8 bond lengths before an absorption will occur at 360 nm (Kuhn, 1949). Therefore our
173 results suggest SOA produced from isoprene photochemical oxidation does not contain products that
174 have extended carbon conjugated chains, consistent with current understanding that isoprene
175 photochemical oxidation products consist of carbonyls, hydroxycarbonyls, diols and organic peroxides
176 (e.g., Nguyen et al., 2011). On the other hand, Lin et al. (2014) has suggested that acidic seeds may
177 promote formation of oligomers through reactive uptake of IEPOX and produced light-absorbing
178 organic aerosols under certain conditions. In our experiments, neither acidic seeds nor excess ammonia
179 are present, which could explain the difference between our observations and those of Lin et al. (2014).
180
181 Compared to isoprene SOA, SOA formed from photochemical oxidation of α-pinene showed slightly
182 higher absorption in the 300-350 nm wavelength range, though the absolute MAC values are still small.
183 We observe a slight increase in the MAC values at wavelengths below 450 nm for the α-pinene SOA

184 formed under high-NO_x conditions relative to that formed in the absence of NO_x. These observations
185 are consistent with other studies that have found minimal light absorption for α-pinene SOA, again
186 indicating that the compounds partitioning to the condensed phase do not have extended conjugation
187 (Henry and Donahue, 2012;Nakayama et al., 2010;Laskin et al., 2014).
188
189 In contrast to the SOA produced from the terpene precursors, aromatic precursors representative of
190 anthropogenic VOCs produce SOA that significantly absorbs light, particularly in the UV wavelength
191 range. Overall, the MAC values of the SOA produced from both TMB and toluene are much higher than
192 biogenic SOA, for both NO_x-free and high-NO_x conditions (Figure 2). Lambe et al. (2013) has
193 suggested that the conjugated double bonds retained in oxidation products of aromatic precursors are
194 likely to contribute to absorption in the ultraviolet to near visible range. SOA formed from non-aromatic
195 precursors, on the other hand, did not show strong light absorption in the ultraviolet/visible range due to
196 lack of extended conjugated double bond networks.
197
198 For both toluene and TMB SOA, high NO_x products show substantially higher light absorption than low
199 NO_x. Shown in figures 1 and 2, aromatic SOA formed under high NO_x conditions have much higher
200 MAC values, both in the UV and in the visible. Several studies, based upon both chamber and field
201 observations, have suggested that nitrogen-containing molecules are strong light absorbers (i.e.,
202 Nakayama et al., 2013;Liu et al., 2015b;Zhang et al., 2011;Lin et al., 2015b). In a companion study, we
203 reported detailed characterization of the most prominent BrC chromophores in toluene-SOA formed
204 under both NO_x-free and high-NO_x conditions by deploying liquid chromatography combined with a

UV/vis detector and high-resolution mass spectrometry (LC-UV/Vis-ESI/HRMS) (Lin et al., 2015b). Samples of toluene-SOA produced under high-NO_x and NO_x-free conditions have substantially different chemical compositions. In high-NO_x SOA, we identified 15 nitro-aromatic compounds, including nitrocatechol, dinitrocatechol and nitrophenol, the total absorbance of which accounts for 60% and 41% of the overall absorbance in the wavelength ranges of 300-400nm and 400-500nm, respectively (Lin et al., 2015b). In contrast, photooxidation products observed in NO_x-free SOA are dominated by non-aromatic compounds with high degree of saturation, which did not show substantial light absorption in the UV/Vis range. Similar to toluene SOA, TMB SOA produced under high-NO_x conditions contains nitrogen-containing compounds in contrast to NO_x-free SOA, which explains the difference in light-absorbing properties (Liu et al., 2012).

For similar reaction conditions, the TMB-derived SOA are less absorptive than the toluene SOA. The difference in the light absorption properties between toluene SOA and TMB SOA may be explained by the difference in the production of nitrophenols. Sato et al. (2012) showed that nitrophenols were not detected in the TMB SOA, possibly due to the fact that NO_2 addition to the phenoxy radical formed in reaction of TMB with OH is inhibited. Our measurement is consistent with this hypothesis and infers that nitro-aromatics such as nitrophenols are the main sources of light absorption for the aromatic SOA.

The MAC values of SOA produced from aromatic VOCs are comparable to those of other light-absorbing material relevant to atmospheric aerosol particles, such as fulvic acid. Shown in Figure 3a, the blue shaded area represents the measured MAC range of SOA produced in the toluene+NO_x

226 experiments, with the MAC of Suwannee River fulvic acid as a reference. Over the wavelength range
227 380-480 nm, toluene SOA has higher MAC values than fulvic acid. Since fulvic acid is often cited as a
228 surrogate of strong light-absorbing atmospheric BrC associated with biomass burning, this comparison
229 shows that light absorption by BrC produced from anthropogenic VOCs can be significant under certain
230 photochemical condition, consistent with high MAC values measured previously in urban environments
231 when biomass burning impacts were low (e.g., Zhang et al., 2011, 2013; Liu et al., 2013).
232
233 3.2 Mixed precursor experiments
234 Results from laboratory studies have shown that the addition of isoprene reduced the BrC absorption of
235 aerosols formed from toluene+α-pinene mixtures(Jaoui et al., 2008). The lower absorption was
236 attributed to decreased organic aerosol yields (e.g., lower amounts of light-absorbing SOA were formed)
237 (Jaoui et al., 2008). From ambient observations, Zhang et al. (2011) reported contrasting light
238 absorption properties in two urban environments. Fresh SOA in LA displayed much higher light-
239 absorption presumably because of the anthropogenic-dominated environment, while Atlanta aerosols
240 formed from a mix of anthropogenic and biogenic (isoprene) VOC precursors had a 4-6 times lower
241 MAC value. Hecobian et al. (2010) measured the light absorption of water-soluble organic carbon
242 (WSOC) in Atlanta in different seasons and found that the winter WSOC has a ~3 times higher MAC
243 than summer, due to a higher fraction of organic aerosols formed from biogenic VOCs in summer.
244 Using summer-time samples collected in Atlanta, Liu et al. (2013) reported a significantly higher BrC
245 MAC value that was associated with primary anthropogenic emissions, compared to the lower MAC
246 value observed at sites with local anthropogenic emissions on top of regional biogenic-dominant

emissions. To investigate whether isoprene photooxidation products enhance or inhibit absorption of aromatic SOA, we conducted two mixed-precursor experiments. Figure 4 shows the comparison of MAC values at 365 nm of SOA formed from single precursor and from mixed isoprene and aromatic VOCs, under high-NO_x conditions. In both isoprene/toluene and isoprene/TMB experiments, the SOA formed has lower MAC values than those formed from the pure aromatics alone. Qualitatively, this is the behavior that one would expect, since non-absorbing isoprene SOA will "dilute" the chromophores from the aromatic-derived SOA. To determine whether the total aerosol absorption can be described quantitatively, we first estimate the mass of aromatic- and isoprene-derived SOA (Table S2) using a partitioning model described in section 2.1. We then calculate predicted aerosol MAC values as the mass-weighted average of the MAC values measured for the pure isoprene- and aromatic- derived SOA species. Figure 4 shows a comparison of the measured and predicted mixed-precursor SOA optical properties. The predicted MAC values are 31%-55% lower than the measurements, a difference that is likely outside of the measurement uncertainty. There are several potential explanations for the difference between the predicted and observed MAC values. First, it is possible that SOA formation is not well-described by partitioning theory. One potential source of error in our calculation is that we assume isoprene and aromatic SOA are fully miscible in one another; however, we note that the total predicted SOA mass is within 10% of the observed SOA mass and hence the underprediction of the MAC values cannot be explained by this error. A second possibility is that the partitioning model underestimates the mass of aromatic SOA that has condensed into the mixed-phase particles. Studies have shown that gas-phase wall loss of toluene reaction products can be significant under certain conditions in batch-mode experiments (Zhang et al., 2014). The SOA yield parameterizations are based

on data collected in the absence of seed particles, in which case gas-phase wall loss could be significant. However, isoprene reacts much more quickly than toluene (Figure S2); therefore isoprene SOA should form first and provide surface area which should mitigate gas-phase wall loss of the toluene reaction products. Because no seed particles were present in the pure toluene experiments, we would expect those yield values to be biased low relative to the toluene yield in the mixed precursor experiments, thus potentially explain the underprediction of MAC values. A third possibility is that organic peroxides and alcohols, which were shown to be the dominant component of isoprene SOA (Krechmer et al., 2015), may react with toluene SOA components to produce oligomers capable of absorbing in the UV/VIS that are not present in the single-precursor SOA particles. Examination of the AMS spectra in the mixed experiments and comparison to the spectra of the pure aromatic- and isoprene- SOA were inconclusive in providing evidence of this hypothesis. Samples were not collected for detailed analysis by LC-UV/Vis-ESI/HRMS. Therefore, at this time we can't conclusively explain the apparent absorption enhancements we observe.

3.3 Effect of Relative Humidity on Light Absorption by aromatic SOA

In order to investigate the effect of RH on SOA light absorption, both toluene and TMB photo-oxidation experiments were conducted at fixed VOC and NO_x values but variable RH levels (Table 1). Figure 5 illustrates the light absorption spectra of toluene- and TMB-derived SOA as a function of experimental RH. The data shown here were from samples collected at a photolysis time of 200 minutes which corresponds to the time when light absorption reached its highest value. In both TMB and toluene experiments, SOA generated under dry conditions (RH <5%) displayed significantly lower MACs than

289 SOA formed at RH>30%. SOA formed at 30, 50 and 80% RH have similar light absorption to one
290 another. Thus moderate RH enhances the MAC values by a factor of 1.33 at 365 nm and further
291 increases in RH have no effect. An overview of toluene-SOA molecular compositions was analyzed by
292 nano-DESI/HRMS(Lin et al., 2015b), and showed that a large number of nitrogen containing
293 compounds (CHON) were produced under moderate RH condition (Figure S3). The difference in
294 molecular compositions suggest that low RH inhibited the formation of nitrogen-containing compounds,
295 which have been shown to be major light absorbers in toluene-SOA formed in the presence of
296 NO_x(Nakayama et al., 2013;Liu et al., 2015b;Zhang et al., 2011;Lin et al., 2015b).
297
298 We are unable to identify any gas-phase reactions in the toluene photolysis mechanism directly
299 involving water vapor. Thus, we conclude that RH must be affecting particle-phase reactions that
300 enhance chromophore formation. Several studies have investigated the effect of RH on various particle-
301 phase SOA chemistry and optical properties. Song et al. (2013) found that SOA produced from α-
302 pinene+NO_x+O_3 in the presence of acidic seed aerosols at elevated RH was less light-absorbing than
303 SOA formed under dry conditions, which is opposite of our observations. They suggested that the
304 change in light-absorbing properties might be triggered by evaporation of water, which may have
305 enhanced the acidity of aerosol seeds (Nguyen et al., 2012), thererby promoting oligomerization
306 reactions. Zhong and Jang (2014) investigated the light absorption of BrC formed from wood burning
307 and observed a faster decay of chromophores at higher RH, which they attributed to the decomposition
308 of chromophores by H_2O_2 that is produced by aqueous-phase photooxidation in the presence of elevated
309 water content level. Moderate to high RH may promote heterogeneous reactions, which aids in the

reactive uptake of volatile compounds into aerosols. Cao and Jang (2010) decoupled SOA mass into partitioning and heterogeneous aerosol production in a toluene-NO_x system, and suggested that moderate RH results in a higher fraction of SOA formed via heterogeneous reactions than low RH conditions. Similar effects might be also pertinent to the toluene SOA. Another possible explanation is that SOA formed under low RH conditions may exist in a viscous, semi-solid, or glassy state due to particle-phase oligomerization reactions (Saukko et al., 2012;Shiraiwa et al., 2013) while SOA formed at moderate/high RH would be less viscous. Since only one experiment was conducted under dry condition for each compound it is difficult to draw conclusions, but further investigations are warranted.

3.4 Effect of photochemical aging on light absorption of aromatic SOA

Atmospheric aerosols have a wide range of lifetimes, ranging from hours to days (i.e., Wagstrom and Pandis, 2009). Previous studies have observed a decrease in aerosol absorption with aging in BrC from various sources including biomass burning and SOA formed from aromatics (Forrister et al., 2015;Zhong and Jang, 2011;Lee et al., 2014). We therefore performed several experiments to study the effect of aging on BrC absorption. Figure 6 shows the MAC values at 365 nm as a function of photolysis time for toluene and TMB SOA produced in the presence of NO_x at 30% RH (complete spectra in the wavelength range of 300-700 nm are provided as Figure S4 in SI, with values tabulated in Table S3). We observe a clear decrease in aerosol absorption with aging with MAC values decreasing by ~35% after 400 minutes and >50% after 800 minutes.

Laboratory studies have suggested that photo-bleaching was due to degradation of BrC chromophores (Lee et al., 2014;Zhong and Jang, 2011;Zhong and Jang, 2014). In our observations, the decrease of MAC with aging is accompanied by a decreasing ON-to-OM ratio, shown in Figure 6. Here we define the term ON as the sum of NO, NO_2 and $C_xH_yO_zN_w$ families measured by AMS, to represent organic nitrates formed during the experiments. NO and NO_2 come exclusively from organic nitrates in these experiments. Ammonium is below the instrument detection limit, and the ratio of m/z 30:46 (around 5-6) is indicative of organic nitrate, thus ruling out formation of ammonium nitrate (Farmer et al., 2010). Therefore, the decrease in the aerosol ON:OM with time indicates the loss of ON groups (Figure 6). ON groups have been identified as the strong light absorbers in aromatic SOA formed under high-NO_x conditions, thus the relative decrease in ON fraction relative to OM is consistent with the observed evolution in OA light absorption.

This observed loss of ON could be caused by photolysis and/or hydrolysis of ON groups. Lee et al. (2014) has observed a substantial decline in the double bond equivalent (DBE) values upon photolysis of aromatic SOA, and suggested that the decrease in SOA light absorption and chemical composition was due to photolysis. On the other hand, Liu et al. (2012) suggested that particle-phase hydrolysis could substantially reduce ON group concentration, which they also related to a decrease in BrC light absorption. To distinguish between the effects from photolysis and hydrolysis, SOA was allowed to age in the chamber with UV lights off but at elevated RH in several experiments. Shown in figure 7, the MAC values of toluene and TMB SOA are approximately constant with aging despite the elevated RH. Therefore, we conclude that decrease in MAC values are driven primarily by photolysis (i.e.,

photobleaching), which is correlated with loss of ON groups that have been shown in many studies, including our sister study, to be BrC chromophores (Lin et al., 2015b;Liu et al., 2015b;Zhang et al., 2013). The effect of RH is less clear, with the dark experiments suggesting the net effect of water-related processes, such as hydrolysis and oligomerization, is either negligible or tends to slightly enhance BrC light absorption, while comparison of experiments with and without RH (section 3.3) suggesting moderate RH enhances the SOA MAC values.

3.5 Imaginary refractive indices

So far, our discussion focused on mass-normalized absorption based on solution measurements, which is not directly relatable to light absorption by aerosol particles. Therefore, we derive the imaginary refractive index, *k*, from spectroscopic data, which can be incorporated into climate models. The *k* value is derived using equation 2:

$$k = \frac{\rho_p \lambda \cdot Abs(\lambda)}{4\pi \cdot OM} = \frac{\rho_p \lambda}{4\pi} MAC(\lambda) \quad (2)$$

where *Abs(λ)* is the solution absorption at a given wavelength, OM is the organic mass extracted in solution, and ρ_p is the density of organic aerosols. The density of organic aerosols was calculated by comparing the volume-weighted mobility size measured by SMPS and the mass-weighted aerodynamic size distribution measured by AMS (DeCarlo et al., 2004). A density of 1.25±0.3 g cm^{-3} was obtained for SOA produced under NO_x-free conditions, while a density of 1.41±0.2 g cm^{-3} was estimated for SOA produced in high-NO_x experiments. Those density values were employed in equation 2 to estimate *k* values at 365 nm for various types of SOA, which are summarized in Table 2 (k values for the 300-700 nm range are listed in Table S4).

Although α-pinene and isoprene have large contributions to the global SOA budget, they were shown to produce SOA with very small light absorption coefficients under the photochemical conditions we investigated, which agrees with literature data (i.e., Nakayama et al., 2010;Lang-Yona et al., 2010). The SOA compounds produced are dominated by carbonyl, carboxyl, and hydroxyl functional groups, which do not have strong electronic transitions in the UV/Vis range. As a result, those biogenic SOA particles are expected to have a mostly cooling effect on global radiative balance. However, studies have shown that biogenic SOA can be converted into BrC via reactions with dissolved ammonia (Updyke et al., 2012;Laskin et al., 2014), or by monoterpene SOA formed from nighttime reactions with NO_3 radical (Washenfelder et al., 2015). Furthermore, it has been demonstrated that reactive uptake of IEPOX into acidic aerosols produce BrC (Lin et al., 2014b), which may have substantial impacts on specific regions with elevated ammonia levels and/or active IEPOX chemistry.

In the present study, the SOA generated from the photooxidation of aromatic VOC precursors, particularly toluene, were found to have significant absorption in the UV/Vis range when formed in the presence of NO_x. Toluene-SOA formed under high-NO_x conditions has a *k* value ranging from 0.019 to 0.047 at 365 nm, and 0.011-0.033 at 405 nm. Shown in Figure 3b, the k values are in good agreement with the measurement by Nakayama et al. (2010), where reported k values were 0.047 at 355 nm and 0.007 at 532 nm. The k values reported by Zhong and Jang (2011) and Liu et al. (2015b) are close to the lower limit from this work, the former reported a k value of 0.0214 at 350 nm, and the latter reported a range of 0.022-0.033 at 320 nm. However, the *k* values derived in this work are substantially higher

than those in Nakayama et al. (2013), which reported *k* values ranging from 0.0018 to 0.0072 at 405 nm. A possible explanation is the difference in NO_x levels among the experiments; Zhong and Jang (2011) and Nakayama et al. (2013) studies were conducted at NO_x levels lower than 1 ppmv, which are lower than employed in our study. Nakayama et al. (2013) has reported that light absorption of SOA has a dependence on NO_x, that MAC increases with NO_x , which likely also explains the higher k values reported by earlier work from the same group (Nakayama et al., 2010). Another potentially important difference among the experiments is the RH, with Nakayama 2013 and the Liu studies conducted under dry conditions(Nakayama et al., 2013;Liu et al., 2015b). From what we have observed, moderate RH could enhance the light absorption of BrC.

4. Conclusions and Atmospheric Implications

Among ambient studies reporting BrC light absorption, high MAC values are almost exclusively reported for aerosols attributed to biomass burning (Kirchstetter et al., 2004;Hoffer et al., 2006;Alexander et al., 2008;Dinar et al., 2008;Chakrabarty et al., 2010;Lack et al., 2013), and the limited number of models that include BrC generally use biomass burning aerosol optical properties as high-absorption references (Lin et al., 2014a;Feng et al., 2013). Our results suggest that organic aerosols formed from certain anthropogenic VOC precursors also display efficient light absorption. Specifically, the MAC values obtained from the toluene+high-NO_x experiment were comparable to that of fulvic acid, which has been used as model compounds for biomass burning HULIS(Dinar et al., 2006;Brooks et al., 2004;Chan and Chan, 2003;Fuzzi et al., 2001;Samburova et al., 2005). The results suggest that in

addition to BrC from biomass burning, the photooxidation of anthropogenic precursors can also have significant impacts on light absorption at wavelengths that drive photochemical reactions.

BrC observed in urban environments has large variations in reported MAC values, and our mixed-precursor experiments may provide some explanations for the observed variation. From our measurements, SOA formed from mixtures of isoprene+aromatic VOC have lower MAC values than those formed from the pure aromatics, suggesting that isoprene photooxidation products dilute light-absorbing compounds. Therefore, it is possible that some of the variance in BrC properties between urban sites can be explained by the presence or absence of biogenic emissions. In addition, our results suggested that NO_x concentration, RH level, and photolysis time have considerable influences on the formation and decay of light-absorbing compounds. Similar light-absorbing compounds have been identified in certain SOA samples originating from biomass burning (Desyaterik et al., 2013;Iinuma et al., 2010); since substantial variations in SOA formation in biomass burning plumes have been observed both chemically and physically due to fuel types and fire aging conditions (Hennigan et al., 2011), we cannot simply assume similar effects of those parameters on SOA produced from biomass burning emissions. Thus the result suggests that we should revisit how SOA is treated in climate models, especially in urban areas. Several current regional and global models include NO_x-dependent SOA yield (Lane et al., 2008;Farina et al., 2010;Ahmadov et al., 2012); accurately parameterizing BrC formation from SOA will require a similar strategy.

Acknowledgements

Authors acknowledge support by the Laboratory Directed Research and Development funds of Pacific Northwest National Laboratory (PNNL). A portion of this study was performed at the William R. Wiley Environmental Molecular Sciences Laboratory, a national scientific user facility sponsored by the DOE's Office of Biological and Environmental Research and located at PNNL. PNNL is operated for the U.S. Department of Energy by Battelle Memorial Institute under Contract No. DE-AC06-76RLO 1830.

References

Ahmadov, R., McKeen, S. A., Robinson, A. L., Bahreini, R., Middlebrook, A. M., de Gouw, J. A., Meagher, J., Hsie, E. Y., Edgerton, E., Shaw, S., and Trainer, M.: A volatility basis set model for summertime secondary organic aerosols over the eastern United States in 2006, Journal of Geophysical Research: Atmospheres, 117, D06301, 10.1029/2011JD016831, 2012.

Alexander, D. T. L., Crozier, P. A., and Anderson, J. R.: Brown carbon spheres in East Asian outflow and their optical properties, Science, 321, 833-836, DOI 10.1126/science.1155296, 2008.

Andreae, M. O., and Gelencsér, A.: Black carbon or brown carbon? The nature of light-absorbing carbonaceous aerosols, Atmos. Chem. Phys., 6, 3131-3148, 10.5194/acp-6-3131-2006, 2006.

Bikkina, S., and Sarin, M. M.: Light absorbing organic aerosols (brown carbon) over the tropical Indian Ocean: impact of biomass burning emissions, Environ Res Lett, 8, 044042, 2013.

Bond, T. C., Doherty, S. J., Fahey, D. W., Forster, P. M., Berntsen, T., DeAngelo, B. J., Flanner, M. G., Ghan, S., Kärcher, B., Koch, D., Kinne, S., Kondo, Y., Quinn, P. K., Sarofim, M. C., Schultz, M. G., Schulz, M., Venkataraman, C., Zhang, H., Zhang, S., Bellouin, N., Guttikunda, S. K., Hopke, P. K., Jacobson, M. Z., Kaiser, J. W., Klimont, Z., Lohmann, U., Schwarz, J. P., Shindell, D., Storelvmo, T., Warren, S. G., and Zender, C. S.: Bounding the role of black carbon in the climate system: A scientific assessment, Journal of Geophysical Research: Atmospheres, 118, 5380-5552, 10.1002/jgrd.50171, 2013.

Bones, D. L., Henricksen, D. K., Mang, S. A., Gonsior, M., Bateman, A. P., Nguyen, T. B., Cooper, W. J., and Nizkorodov, S. A.: Appearance of strong absorbers and fluorophores in limonene-O3 secondary organic aerosol due to NH4+-mediated chemical aging over long time scales, Journal of Geophysical Research: Atmospheres, 115, D05203, 10.1029/2009JD012864, 2010.

Brooks, S. D., DeMott, P. J., and Kreidenweis, S. M.: Water uptake by particles containing humic materials and mixtures of humic materials with ammonium sulfate, Atmos Environ, 38, 1859-1868, http://dx.doi.org/10.1016/j.atmosenv.2004.01.009, 2004.

Cao, G., and Jang, M.: An SOA Model for Toluene Oxidation in the Presence of Inorganic Aerosols, Environ Sci Technol, 44, 727-733, 10.1021/es901682r, 2010.

Chakrabarty, R. K., Moosmüller, H., Chen, L. W. A., Lewis, K., Arnott, W. P., Mazzoleni, C., Dubey, M. K., Wold, C. E., Hao, W. M., and Kreidenweis, S. M.: Brown carbon in tar balls from smoldering biomass combustion, Atmos. Chem. Phys., 10, 6363-6370, 10.5194/acp-10-6363-2010, 2010.

Chan, M. N., and Chan, C. K.: Hygroscopic Properties of Two Model Humic-like Substances and Their Mixtures with Inorganics of Atmospheric Importance, Environ Sci Technol, 37, 5109-5115, 10.1021/es034272o, 2003.

Chen, Y., and Bond, T. C.: Light absorption by organic carbon from wood combustion, Atmos Chem Phys, 10, 1773-1787, 2010.

Chung, C. E., Ramanathan, V., and Decremer, D.: Observationally constrained estimates of carbonaceous aerosol radiative forcing, Proceedings of the National Academy of Sciences, 109, 11624-11629, 10.1073/pnas.1203707109, 2012.

De Haan, D. O. D., Corrigan, A. L., Smith, K. W., Stroik, D. R., Turley, J. J., Lee, F. E., Tolbert, M. A., Jimenez, J. L., Cordova, K. E., and Ferrell, G. R.: Secondary Organic Aerosol-Forming Reactions of Glyoxal with Amino Acids, Environ Sci Technol, 43, 2818-2824, 10.1021/es803534f, 2009.

DeCarlo, P. F., Slowik, J. G., Worsnop, D. R., Davidovits, P., and Jimenez, J. L.: Particle Morphology and Density Characterization by Combined Mobility and Aerodynamic Diameter Measurements. Part 1: Theory, Aerosol Sci Tech, 38, 1185-1205, 10.1080/027868290903907, 2004.

DeCarlo, P. F., Kimmel, J. R., Trimborn, A., Northway, M. J., Jayne, J. T., Aiken, A. C., Gonin, M., Fuhrer, K., Horvath, T., Docherty, K. S., Worsnop, D. R., and Jimenez, J. L.: Field-Deployable, High-Resolution,

Time-of-Flight Aerosol Mass Spectrometer, Analytical Chemistry, 78, 8281-8289, 10.1021/ac061249n, 2006.
Desyaterik, Y., Sun, Y., Shen, X. H., Lee, T. Y., Wang, X. F., Wang, T., and Collett, J. L.: Speciation of "brown" carbon in cloud water impacted by agricultural biomass burning in eastern China, J Geophys Res-Atmos, 118, 7389-7399, Doi 10.1002/Jgrd.50561, 2013.
Dinar, E., Mentel, T. F., and Rudich, Y.: The density of humic acids and humic like substances (HULIS) from fresh and aged wood burning and pollution aerosol particles, Atmos. Chem. Phys., 6, 5213-5224, 10.5194/acp-6-5213-2006, 2006.
Dinar, E., Abo Riziq, A., Spindler, C., Erlick, C., Kiss, G., and Rudich, Y.: The complex refractive index of atmospheric and model humic-like substances (HULIS) retrieved by a cavity ring down aerosol spectrometer (CRD-AS), Faraday Discuss, 137, 279-295, 10.1039/B703111D, 2008.
Du, Z., He, K., Cheng, Y., Duan, F., Ma, Y., Liu, J., Zhang, X., Zheng, M., and Weber, R.: A yearlong study of water-soluble organic carbon in Beijing II: Light absorption properties, Atmos Environ, 89, 235-241, http://dx.doi.org/10.1016/j.atmosenv.2014.02.022, 2014.
Duarte, R. M. B. O., Pio, C. A., and Duarte, A. C.: Spectroscopic study of the water-soluble organic matter isolated from atmospheric aerosols collected under different atmospheric conditions, Analytica Chimica Acta, 530, 7-14, http://dx.doi.org/10.1016/j.aca.2004.08.049, 2005.
Farina, S. C., Adams, P. J., and Pandis, S. N.: Modeling global secondary organic aerosol formation and processing with the volatility basis set: Implications for anthropogenic secondary organic aerosol, Journal of Geophysical Research: Atmospheres, 115, D09202, 10.1029/2009JD013046, 2010.
Farmer, D. K., Matsunaga, A., Docherty, K. S., Surratt, J. D., Seinfeld, J. H., Ziemann, P. J., and Jimenez, J. L.: Response of an aerosol mass spectrometer to organonitrates and organosulfates and implications for atmospheric chemistry, Proceedings of the National Academy of Sciences, 107, 6670-6675, 10.1073/pnas.0912340107, 2010.
Feng, Y., Ramanathan, V., and Kotamarthi, V. R.: Brown carbon: a significant atmospheric absorber of solar radiation?, Atmos Chem Phys, 13, 8607-8621, DOI 10.5194/acp-13-8607-2013, 2013.
Forrister, H., Liu, J., Scheuer, E., Dibb, J., Ziemba, L., Thornhill, K. L., Anderson, B., Diskin, G., Perring, A. E., Schwarz, J. P., Campuzano-Jost, P., Day, D. A., Palm, B. B., Jimenez, J. L., Nenes, A., and Weber, R. J.: Evolution of Brown Carbon in Wildfire Plumes, Geophysical Research Letters, 42, 4623–4630, 10.1002/2015GL063897, 2015.
Fuzzi, S., Decesari, S., Facchini, M. C., Matta, E., Mircea, M., and Tagliavini, E.: A simplified model of the water soluble organic component of atmospheric aerosols, Geophysical Research Letters, 28, 4079-4082, 10.1029/2001GL013418, 2001.
Galloway, M. M., Chhabra, P. S., Chan, A. W. H., Surratt, J. D., Flagan, R. C., Seinfeld, J. H., and Keutsch, F. N.: Glyoxal uptake on ammonium sulphate seed aerosol: reaction products and reversibility of uptake under dark and irradiated conditions, Atmos. Chem. Phys., 9, 3331-3345, 10.5194/acp-9-3331-2009, 2009.
Guenther, A., Karl, T., Harley, P., Wiedinmyer, C., Palmer, P. I., and Geron, C.: Estimates of global terrestrial isoprene emissions using MEGAN (Model of Emissions of Gases and Aerosols from Nature), Atmos Chem Phys, 6, 3181-3210, 2006.
Guenther, A. B., Jiang, X., Heald, C. L., Sakulyanontvittaya, T., Duhl, T., Emmons, L. K., and Wang, X.: The Model of Emissions of Gases and Aerosols from Nature version 2.1 (MEGAN2.1): an extended and updated framework for modeling biogenic emissions, Geosci. Model Dev., 5, 1471-1492, 10.5194/gmd-5-1471-2012, 2012.
Hecobian, A., Zhang, X., Zheng, M., Frank, N., Edgerton, E. S., and Weber, R. J.: Water-Soluble Organic Aerosol material and the light-absorption characteristics of aqueous extracts measured over the Southeastern United States, Atmos Chem Phys, 10, 5965-5977, DOI 10.5194/acp-10-5965-2010, 2010.

Hennigan, C. J., Miracolo, M. A., Engelhart, G. J., May, A. A., Presto, A. A., Lee, T., Sullivan, A. P., McMeeking, G. R., Coe, H., Wold, C. E., Hao, W. M., Gilman, J. B., Kuster, W. C., de Gouw, J., Schichtel, B. A., Collett Jr, J. L., Kreidenweis, S. M., and Robinson, A. L.: Chemical and physical transformations of organic aerosol from the photo-oxidation of open biomass burning emissions in an environmental chamber, Atmos. Chem. Phys., 11, 7669-7686, 10.5194/acp-11-7669-2011, 2011.

Henry, K. M., and Donahue, N. M.: Photochemical Aging of α-Pinene Secondary Organic Aerosol: Effects of OH Radical Sources and Photolysis, The Journal of Physical Chemistry A, 116, 5932-5940, 10.1021/jp210288s, 2012.

Henze, D. K., Seinfeld, J. H., Ng, N. L., Kroll, J. H., Fu, T. M., Jacob, D. J., and Heald, C. L.: Global modeling of secondary organic aerosol formation from aromatic hydrocarbons: high- vs. low-yield pathways, Atmos. Chem. Phys., 8, 2405-2420, 10.5194/acp-8-2405-2008, 2008.

Hoffer, A., Gelencsér, A., Guyon, P., Kiss, G., Schmid, O., Frank, G. P., Artaxo, P., and Andreae, M. O.: Optical properties of humic-like substances (HULIS) in biomass-burning aerosols, Atmos. Chem. Phys., 6, 3563-3570, 10.5194/acp-6-3563-2006, 2006.

Iinuma, Y., Böge, O., Gräfe, R., and Herrmann, H.: Methyl-Nitrocatechols: Atmospheric Tracer Compounds for Biomass Burning Secondary Organic Aerosols, Environ Sci Technol, 44, 8453-8459, 10.1021/es102938a, 2010.

IPCC fifth assessment report, Weather, 68, 310-310, 2013.

Jaoui, M., Edney, E. O., Kleindienst, T. E., Lewandowski, M., Offenberg, J. H., Surratt, J. D., and Seinfeld, J. H.: Formation of secondary organic aerosol from irradiated α-pinene/toluene/NOx mixtures and the effect of isoprene and sulfur dioxide, Journal of Geophysical Research: Atmospheres, 113, D09303, 10.1029/2007JD009426, 2008.

Kampf, C. J., Jakob, R., and Hoffmann, T.: Identification and characterization of aging products in the glyoxal/ammonium sulfate system – implications for light-absorbing material in atmospheric aerosols, Atmos. Chem. Phys., 12, 6323-6333, 10.5194/acp-12-6323-2012, 2012.

Kieber, R., Whitehead, R., Reid, S., Willey, J., and Seaton, P.: Chromophoric Dissolved Organic Matter (CDOM) In Rainwater, Southeastern North Carolina, USA, Journal of Atmospheric Chemistry, 54, 21-41, 10.1007/s10874-005-9008-4, 2006.

Kirchstetter, T. W., Novakov, T., and Hobbs, P. V.: Evidence that the spectral dependence of light absorption by aerosols is affected by organic carbon, Journal of Geophysical Research: Atmospheres, 109, D21208, 10.1029/2004JD004999, 2004.

Kirchstetter, T. W., and Thatcher, T. L.: Contribution of organic carbon to wood smoke particulate matter absorption of solar radiation, Atmos. Chem. Phys., 12, 6067-6072, 10.5194/acp-12-6067-2012, 2012.

Kleindienst, T. E., Conver, T. S., McIver, C. D., and Edney, E. O.: Determination of Secondary Organic Aerosol Products from the Photooxidation of Toluene and their Implications in Ambient PM2.5, Journal of Atmospheric Chemistry, 47, 79-100, 10.1023/B:JOCH.0000012305.94498.28, 2004.

Krechmer, J. E., Coggon, M. M., Massoli, P., Nguyen, T. B., Crounse, J. D., Hu, W., Day, D. A., Tyndall, G. S., Henze, D. K., Rivera-Rios, J. C., Nowak, J. B., Kimmel, J. R., Mauldin, R. L., Stark, H., Jayne, J. T., Sipilä, M., Junninen, H., St. Clair, J. M., Zhang, X., Feiner, P. A., Zhang, L., Miller, D. O., Brune, W. H., Keutsch, F. N., Wennberg, P. O., Seinfeld, J. H., Worsnop, D. R., Jimenez, J. L., and Canagaratna, M. R.: Formation of Low Volatility Organic Compounds and Secondary Organic Aerosol from Isoprene Hydroxyhydroperoxide Low-NO Oxidation, Environ Sci Technol, 49, 10330−10339, 10.1021/acs.est.5b02031, 2015.

Kuhn, H.: A Quantum-Mechanical Theory of Light Absorption of Organic Dyes and Similar Compounds, The Journal of Chemical Physics, 17, 1198-1212, doi:http://dx.doi.org/10.1063/1.1747143, 1949.

Lack, D. A., Langridge, J. M., Bahreini, R., Cappa, C. D., Middlebrook, A. M., and Schwarz, J. P.: Brown carbon and internal mixing in biomass burning particles, P Natl Acad Sci USA, 109, 14802-14807, DOI 10.1073/pnas.1206575109, 2012.

Lack, D. A., Bahreni, R., Langridge, J. M., Gilman, J. B., and Middlebrook, A. M.: Brown carbon absorption linked to organic mass tracers in biomass burning particles, Atmos Chem Phys, 13, 2415-2422, DOI 10.5194/acp-13-2415-2013, 2013.

Lambe, A. T., Cappa, C. D., Massoli, P., Onasch, T. B., Forestieri, S. D., Martin, A. T., Cummings, M. J., Croasdale, D. R., Brune, W. H., Worsnop, D. R., and Davidovits, P.: Relationship between Oxidation Level and Optical Properties of Secondary Organic Aerosol, Environ Sci Technol, 47, 6349-6357, 10.1021/es401043j, 2013.

Lane, T. E., Donahue, N. M., and Pandis, S. N.: Effect of NOx on Secondary Organic Aerosol Concentrations, Environ Sci Technol, 42, 6022-6027, 10.1021/es703225a, 2008.

Lang-Yona, N., Abo-Riziq, A., Erlick, C., Segre, E., Trainic, M., and Rudich, Y.: Interaction of internally mixed aerosols with light, Phys Chem Chem Phys, 12, 21-31, 10.1039/B913176K, 2010.

Laskin, A., Laskin, J., and Nizkorodov, S. A.: Chemistry of Atmospheric Brown Carbon, Chemical Reviews, 115 (10), 4335–4382, 10.1021/cr5006167, 2015.

Laskin, J., Laskin, A., Nizkorodov, S. A., Roach, P., Eckert, P., Gilles, M. K., Wang, B., Lee, H. J., and Hu, Q.: Molecular Selectivity of Brown Carbon Chromophores, Environ Sci Technol, 48, 12047-12055, 10.1021/es503432r, 2014.

Lee, H. J., Aiona, P. K., Laskin, A., Laskin, J., and Nizkorodov, S. A.: Effect of Solar Radiation on the Optical Properties and Molecular Composition of Laboratory Proxies of Atmospheric Brown Carbon, Environ Sci Technol, 48, 10217-10226, 10.1021/es502515r, 2014.

Leighton, P. A.: Photochemistry of Air Pollution, Academic, San Diego, California, 1961.

Limbeck, A., Kulmala, M., and Puxbaum, H.: Secondary organic aerosol formation in the atmosphere via heterogeneous reaction of gaseous isoprene on acidic particles, Geophysical Research Letters, 30, 1996, 10.1029/2003GL017738, 2003.

Lin, G., Penner, J. E., Flanner, M. G., Sillman, S., Xu, L., and Zhou, C.: Radiative forcing of organic aerosol in the atmosphere and on snow: Effects of SOA and brown carbon, Journal of Geophysical Research: Atmospheres, 119, 2013JD021186, 10.1002/2013JD021186, 2014a.

Lin, P., Laskin, J., Nizkorodov, S. A., and Laskin, A.: Revealing Brown Carbon Chromophores Produced in Reactions of Methylglyoxal with Ammonium Sulfate, Environ Sci Technol, 49 (24), 14257–14266, 10.1021/acs.est.5b03608, 2015a.

Lin, P., Liu, J., Shilling, J. E., Kathmann, S. M., Laskin, J., and Laskin, A.: Molecular characterization of brown carbon (BrC) chromophores in secondary organic aerosol generated from photo-oxidation of toluene, Phys Chem Chem Phys, 17, 23312-23325, 10.1039/C5CP02563J, 2015b.

Lin, Y.-H., Budisulistiorini, S. H., Chu, K., Siejack, R. A., Zhang, H., Riva, M., Zhang, Z., Gold, A., Kautzman, K. E., and Surratt, J. D.: Light-Absorbing Oligomer Formation in Secondary Organic Aerosol from Reactive Uptake of Isoprene Epoxydiols, Environ Sci Technol, 48, 12012-12021, 10.1021/es503142b, 2014b.

Liu, J., Bergin, M., Guo, H., King, L., Kotra, N., Edgerton, E., and Weber, R. J.: Size-resolved measurements of brown carbon in water and methanol extracts and estimates of their contribution to ambient fine-particle light absorption, Atmos Chem Phys, 13, 12389-12404, DOI 10.5194/acp-13-12389-2013, 2013.

Liu, J., Scheuer, E., Dibb, J., Ziemba, L. D., Thornhill, K. L., Anderson, B. E., Wisthaler, A., Mikoviny, T., Devi, J. J., Bergin, M., and Weber, R. J.: Brown carbon in the continental troposphere, Geophysical Research Letters, 41, 2013GL058976, 10.1002/2013GL058976, 2014.

Liu, J., Scheuer, E., Dibb, J., Diskin, G. S., Ziemba, L. D., Thornhill, K. L., Anderson, B. E., Wisthaler, A., Mikoviny, T., Devi, J. J., Bergin, M., Perring, A. E., Markovic, M. Z., Schwarz, J. P., Campuzano-Jost, P., Day, D. A., Jimenez, J. L., and Weber, R. J.: Brown carbon aerosol in the North American continental troposphere: sources, abundance, and radiative forcing, Atmos Chem Phys, 15, 7841-7858, 10.5194/acp-15-7841-2015, 2015a.

Liu, P. F., Abdelmalki, N., Hung, H. M., Wang, Y., Brune, W. H., and Martin, S. T.: Ultraviolet and visible complex refractive indices of secondary organic material produced by photooxidation of the aromatic compounds toluene and m-xylene, Atmos. Chem. Phys., 15, 1435-1446, 10.5194/acp-15-1435-2015, 2015b.

Liu, S., Shilling, J. E., Song, C., Hiranuma, N., Zaveri, R. A., and Russell, L. M.: Hydrolysis of Organonitrate Functional Groups in Aerosol Particles, Aerosol Sci Tech, 46, 1359-1369, 10.1080/02786826.2012.716175, 2012.

Lukács, H., Gelencsér, A., Hammer, S., Puxbaum, H., Pio, C., Legrand, M., Kasper-Giebl, A., Handler, M., Limbeck, A., Simpson, D., and Preunkert, S.: Seasonal trends and possible sources of brown carbon based on 2-year aerosol measurements at six sites in Europe, Journal of Geophysical Research: Atmospheres, 112, D23S18, 10.1029/2006JD008151, 2007.

Mohr, C., Lopez-Hilfiker, F. D., Zotter, P., Prévôt, A. S. H., Xu, L., Ng, N. L., Herndon, S. C., Williams, L. R., Franklin, J. P., Zahniser, M. S., Worsnop, D. R., Knighton, W. B., Aiken, A. C., Gorkowski, K. J., Dubey, M. K., Allan, J. D., and Thornton, J. A.: Contribution of Nitrated Phenols to Wood Burning Brown Carbon Light Absorption in Detling, United Kingdom during Winter Time, Environ Sci Technol, 47, 6316-6324, 10.1021/es400683v, 2013.

Moise, T., Flores, J. M., and Rudich, Y.: Optical Properties of Secondary Organic Aerosols and Their Changes by Chemical Processes, Chemical Reviews, 115 (10), 4400–4439 10.1021/cr5005259, 2015.

Nakayama, T., Matsumi, Y., Sato, K., Imamura, T., Yamazaki, A., and Uchiyama, A.: Laboratory studies on optical properties of secondary organic aerosols generated during the photooxidation of toluene and the ozonolysis of α-pinene, Journal of Geophysical Research: Atmospheres, 115, D24204, 10.1029/2010JD014387, 2010.

Nakayama, T., Sato, K., Matsumi, Y., Imamura, T., Yamazaki, A., and Uchiyama, A.: Wavelength and NOx dependent complex refractive index of SOAs generated from the photooxidation of toluene, Atmos. Chem. Phys., 13, 531-545, 10.5194/acp-13-531-2013, 2013.

Ng, N. L., Kroll, J. H., Chan, A. W. H., Chhabra, P. S., Flagan, R. C., and Seinfeld, J. H.: Secondary organic aerosol formation from m-xylene, toluene, and benzene, Atmos. Chem. Phys., 7, 3909-3922, 10.5194/acp-7-3909-2007, 2007.

Nguyen, T. B., Laskin, J., Laskin, A., and Nizkorodov, S. A.: Nitrogen-Containing Organic Compounds and Oligomers in Secondary Organic Aerosol Formed by Photooxidation of Isoprene, Environ Sci Technol, 45, 6908-6918, Doi 10.1021/Es201611n, 2011.

Nguyen, T. B., Lee, P. B., Updyke, K. M., Bones, D. L., Laskin, J., Laskin, A., and Nizkorodov, S. A.: Formation of nitrogen- and sulfur-containing light-absorbing compounds accelerated by evaporation of water from secondary organic aerosols, Journal of Geophysical Research. Atmospheres, 117, D01207, http://dx.doi.org/10.1029/2011JD016944, 2012.

Nguyen, T. B., Laskin, A., Laskin, J., and Nizkorodov, S. A.: Brown carbon formation from ketoaldehydes of biogenic monoterpenes, Faraday Discuss, 165, 473-494, 10.1039/C3FD00036B, 2013.

Odum, J. R., Hoffmann, T., Bowman, F., Collins, D., Flagan, R. C., and Seinfeld, J. H.: Gas/Particle Partitioning and Secondary Organic Aerosol Yields, Environ Sci Technol, 30, 2580-2585, 10.1021/es950943+, 1996.

Pankow, J. F.: An absorption model of gas/particle partitioning of organic compounds in the atmosphere, Atmos Environ, 28, 185-188, http://dx.doi.org/10.1016/1352-2310(94)90093-0, 1994.

Petzold, A., Ogren, J. A., Fiebig, M., Laj, P., Li, S. M., Baltensperger, U., Holzer-Popp, T., Kinne, S., Pappalardo, G., Sugimoto, N., Wehrli, C., Wiedensohler, A., and Zhang, X. Y.: Recommendations for reporting "black carbon" measurements, Atmos. Chem. Phys., 13, 8365-8379, 10.5194/acp-13-8365-2013, 2013.

Powelson, M. H., Espelien, B. M., Hawkins, L. N., Galloway, M. M., and De Haan, D. O.: Brown Carbon Formation by Aqueous-Phase Carbonyl Compound Reactions with Amines and Ammonium Sulfate, Environ Sci Technol, 48, 985-993, Doi 10.1021/Es4038325, 2014.

Presto, A. A., and Donahue, N. M.: Investigation of α-Pinene + Ozone Secondary Organic Aerosol Formation at Low Total Aerosol Mass, Environ Sci Technol, 40, 3536-3543, 10.1021/es052203z, 2006.

Samburova, V., Zenobi, R., and Kalberer, M.: Characterization of high molecular weight compounds in urban atmospheric particles, Atmos. Chem. Phys., 5, 2163-2170, 10.5194/acp-5-2163-2005, 2005.

Sareen, N., Schwier, A. N., Shapiro, E. L., Mitroo, D., and McNeill, V. F.: Secondary organic material formed by methylglyoxal in aqueous aerosol mimics, Atmos. Chem. Phys., 10, 997-1016, 10.5194/acp-10-997-2010, 2010.

Sato, K., Takami, A., Kato, Y., Seta, T., Fujitani, Y., Hikida, T., Shimono, A., and Imamura, T.: AMS and LC/MS analyses of SOA from the photooxidation of benzene and 1,3,5-trimethylbenzene in the presence of NOx: effects of chemical structure on SOA aging, Atmos. Chem. Phys., 12, 4667-4682, 10.5194/acp-12-4667-2012, 2012.

Saukko, E., Lambe, A. T., Massoli, P., Koop, T., Wright, J. P., Croasdale, D. R., Pedernera, D. A., Onasch, T. B., Laaksonen, A., Davidovits, P., Worsnop, D. R., and Virtanen, A.: Humidity-dependent phase state of SOA particles from biogenic and anthropogenic precursors, Atmos. Chem. Phys., 12, 7517-7529, 10.5194/acp-12-7517-2012, 2012.

Shapiro, E. L., Szprengiel, J., Sareen, N., Jen, C. N., Giordano, M. R., and McNeill, V. F.: Light-absorbing secondary organic material formed by glyoxal in aqueous aerosol mimics, Atmos. Chem. Phys., 9, 2289-2300, 10.5194/acp-9-2289-2009, 2009.

Shiraiwa, M., Zuend, A., Bertram, A. K., and Seinfeld, J. H.: Gas-particle partitioning of atmospheric aerosols: interplay of physical state, non-ideal mixing and morphology, Phys Chem Chem Phys, 15, 11441-11453, 10.1039/C3CP51595H, 2013.

Song, C., Gyawali, M., Zaveri, R. A., Shilling, J. E., and Arnott, W. P.: Light absorption by secondary organic aerosol from α-pinene: Effects of oxidants, seed aerosol acidity, and relative humidity, Journal of Geophysical Research: Atmospheres, 118, 11741-11749, 10.1002/jgrd.50767, 2013.

Updyke, K. M., Nguyen, T. B., and Nizkorodov, S. A.: Formation of brown carbon via reactions of ammonia with secondary organic aerosols from biogenic and anthropogenic precursors, Atmos Environ, 63, 22-31, DOI 10.1016/j.atmosenv.2012.09.012, 2012.

Wagstrom, K. M., and Pandis, S. N.: Determination of the age distribution of primary and secondary aerosol species using a chemical transport model, Journal of Geophysical Research: Atmospheres, 114, D14303, 10.1029/2009JD011784, 2009.

Washenfelder, R. A., Attwood, A. R., Brock, C. A., Guo, H., Xu, L., Weber, R. J., Ng, N. L., Allen, H. M., Ayres, B. R., Baumann, K., Cohen, R. C., Draper, D. C., Duffey, K. C., Edgerton, E., Fry, J. L., Hu, W. W., Jimenez, J. L., Palm, B. B., Romer, P., Stone, E. A., Wooldridge, P. J., and Brown, S. S.: Biomass burning dominates brown carbon absorption in the rural southeastern United States, Geophysical Research Letters, 42, 2014GL062444, 10.1002/2014GL062444, 2015.

Zarzana, K. J., De Haan, D. O., Freedman, M. A., Hasenkopf, C. A., and Tolbert, M. A.: Optical Properties of the Products of α-Dicarbonyl and Amine Reactions in Simulated Cloud Droplets, Environ Sci Technol, 46, 4845-4851, 10.1021/es2040152, 2012.

712 Zhang, X., Lin, Y.-H., Surratt, J. D., Zotter, P., Prévôt, A. S. H., and Weber, R. J.: Light-absorbing soluble
713 organic aerosol in Los Angeles and Atlanta: A contrast in secondary organic aerosol, Geophysical
714 Research Letters, 38, L21810, 10.1029/2011GL049385, 2011.
715 Zhang, X., Lin, Y.-H., Surratt, J. D., and Weber, R. J.: Sources, Composition and Absorption Ångström Exponent
716 of Light-absorbing Organic Components in Aerosol Extracts from the Los Angeles Basin, Environ Sci
717 Technol, 47, 3685-3693, 10.1021/es305047b, 2013.
718 Zhong, M., and Jang, M.: Light absorption coefficient measurement of SOA using a UV–Visible spectrometer
719 connected with an integrating sphere, Atmos Environ, 45, 4263-4271,
720 http://dx.doi.org/10.1016/j.atmosenv.2011.04.082, 2011.
721 Zhong, M., and Jang, M.: Dynamic light absorption of biomass-burning organic carbon photochemically aged
722 under natural sunlight, Atmos. Chem. Phys., 14, 1517-1525, 10.5194/acp-14-1517-2014, 2014.

723

724 Table 1. Summary of experiments and experimental conditions described in this work.

Experiment	Experiment type	VOC	Initial VOC concentration (ppb)	Initial NO (ppb)	RH (%)
1	1	isoprene	359.37	<1 (NO_x-free)	30
2	1	α-pinene	22.73	<1 (NO_x-free)	30
3	1	TMB	316.30	<1 (NO_x-free)	30
4	1	toluene	339.92	<1 (NO_x-free)	30
5	2	isoprene	311.45	1754.67 (high-NO_x)	30
6	2	α-pinene	45.45	466.09 (high-NO_x)	30
7	2	TMB	289.94	1589.6 (high-NO_x)	30
8	2	toluene	317.26	1800 (high-NO_x)	30
9	2	Isoprene+TMB	178.51+123.71	1800 (high-NO_x)	30
10	2	Isoprene+toluene	158.09+106.43	1800 (high-NO_x)	30
11	3	TMB	263.58	1500 (high-NO_x)	30
12	3	toluene	339.92	1900 (high-NO_x)	30
13	4	TMB	263.58	1800 (high-NO_x)	<5
14	4	TMB	263.58	1800 (high-NO_x)	50
15	4	TMB	263.58	1800 (high-NO_x)	80
16	4	Toluene	396	1800 (high-NO_x)	<5
17	4	Toluene	300	1800 (high-NO_x)	50
18	4	Toluene	339.92	1800 (high-NO_x)	80

725

726

727 Table 2. Derived imaginary part of refractive index (k) of brown carbon formed from various VOC
728 precursors at 365 nm. Tabulated values are $k \times 10^3$.

	NO_x-free	High-NO_x
Isoprene	0.029	0.196
α-pinene	0	1.15
TMB	0.967	6.028-9.899
toluene	0.461	19.48-46.87

729

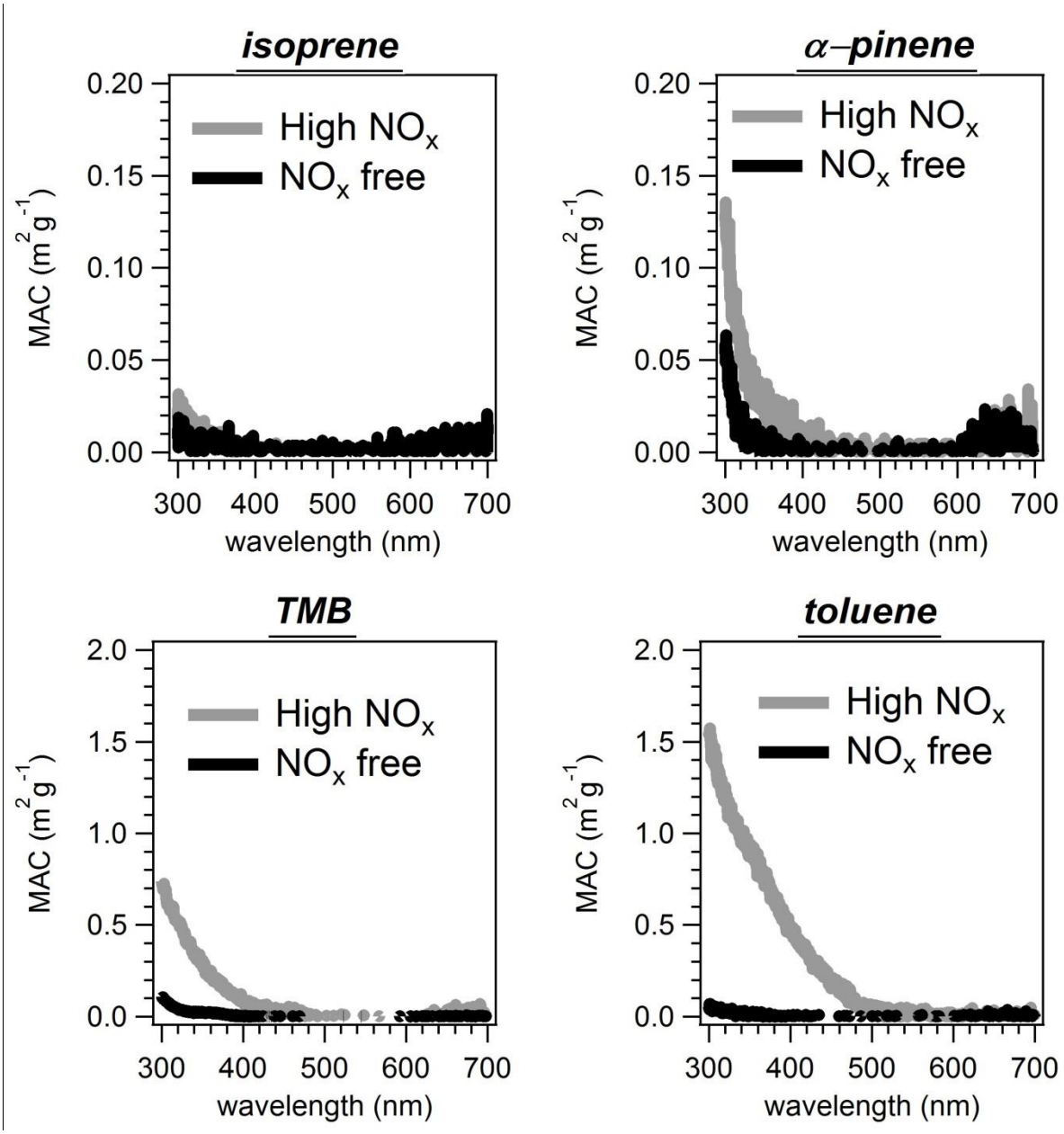

Figure 1. MAC values for SOA formed under NO_x-free and high-NO_x conditions, from isoprene, α-pinene, TMB, and toluene. Note the 10× difference in scale between the terpene and aromatic precursors. The MAC values shown in this figure are tabulated in the supplementary material (Table S1).

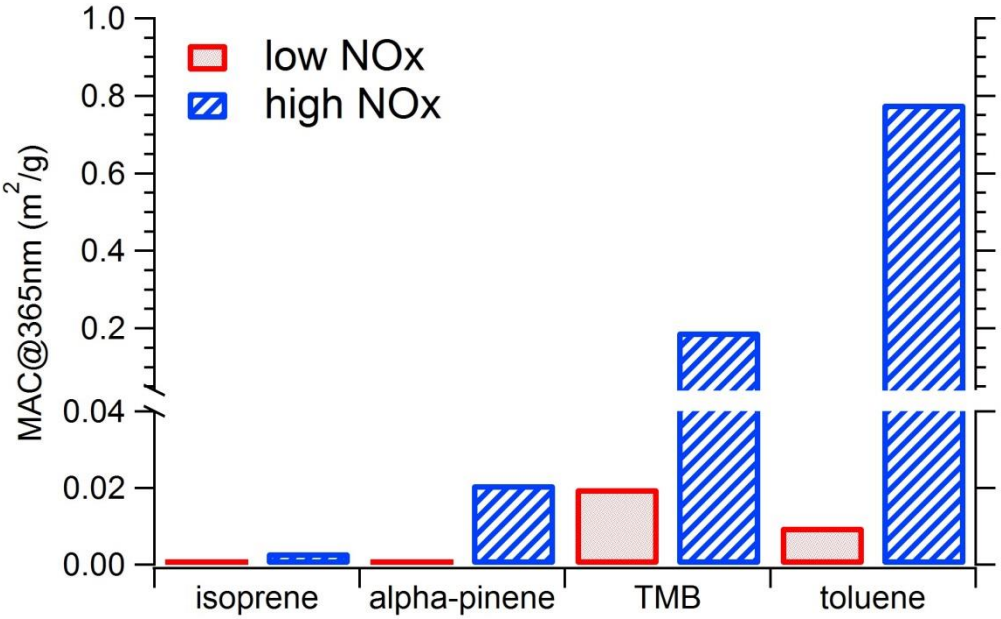

736

737 Figure 2. Comparison of MAC from various types of SOA, at a wavelength of 365 nm.

738

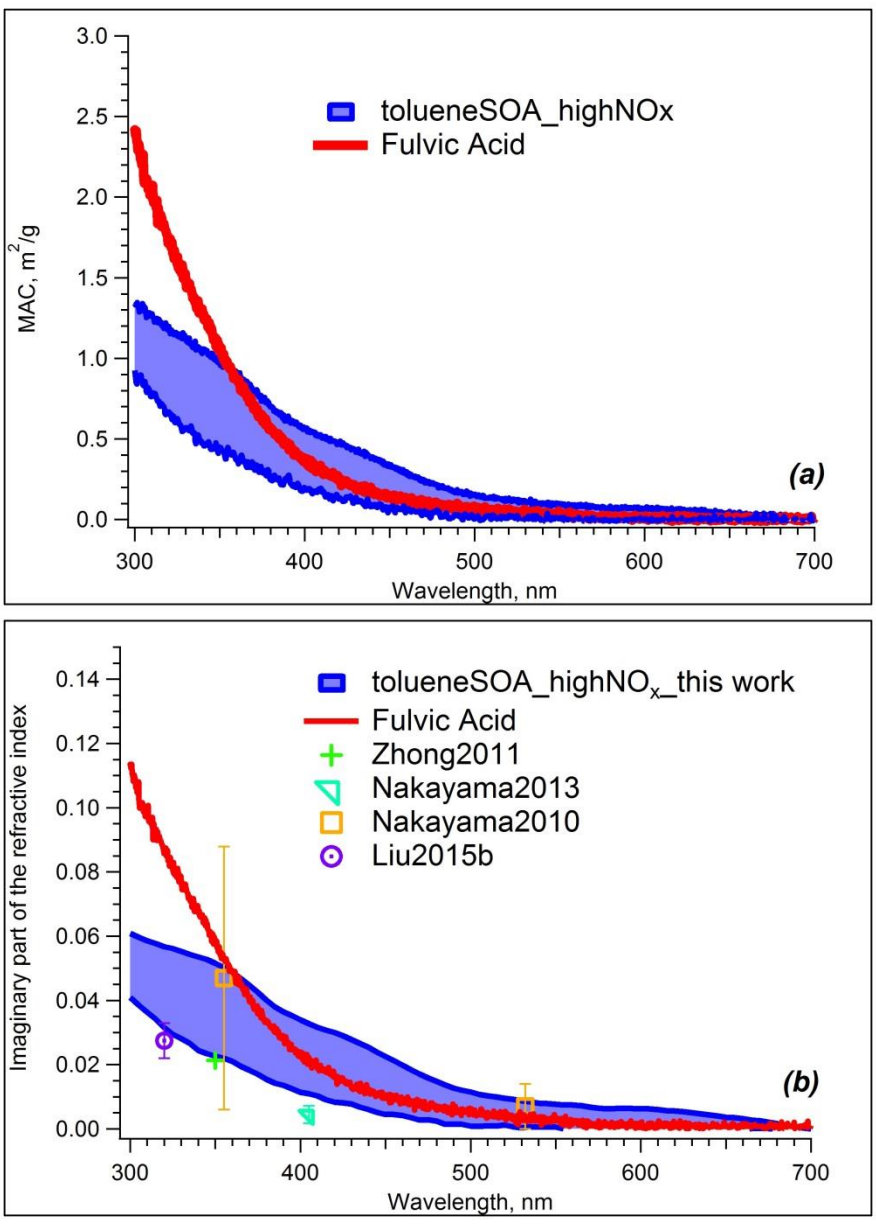

Figure 3. (a) MAC values of Suwanee River fulvic acid (SRFA), and toluene-SOA formed at different high-NO_x conditions. (b) Imaginary part of the refractive index, k, derived from toluene high-NO_x SOA measurements through the 300-700 nm range, with SRFA and literature data as references (Nakayama et al., 2010;Nakayama et al., 2013;Liu et al., 2015b;Zhong and Jang, 2011). SRFA k values were estimated assuming a density of 1.47 g cm^{-3} (Dinar et al., 2006).

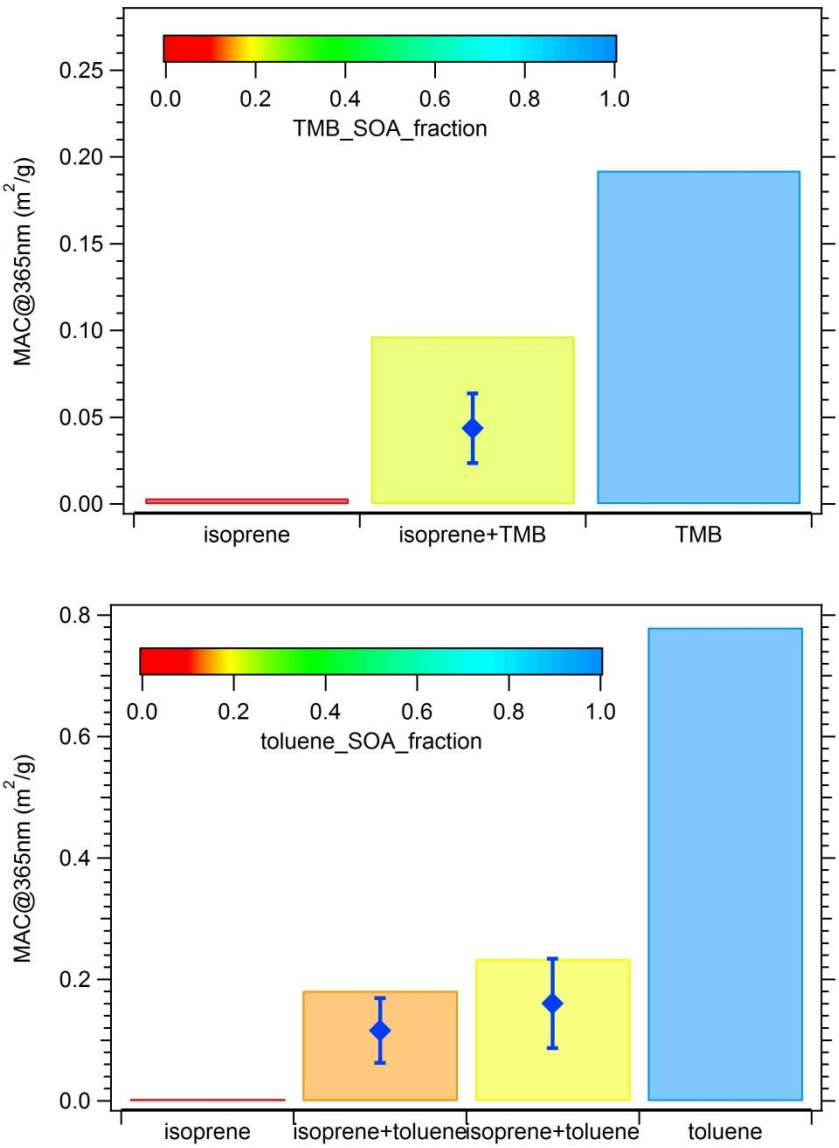

746

747 Figure 4. Comparison of MAC values from single-precursor and mixed precursor experiments. Bars
748 represent the MAC values at 365 nm from measurements, and are color-coded by the mass fraction of
749 aromatic SOA. The blue diamonds represent the predicted MAC values based on the modeled fraction
750 of isoprene SOA and aromatic SOA, with error bars indicating the uncertainty.

751

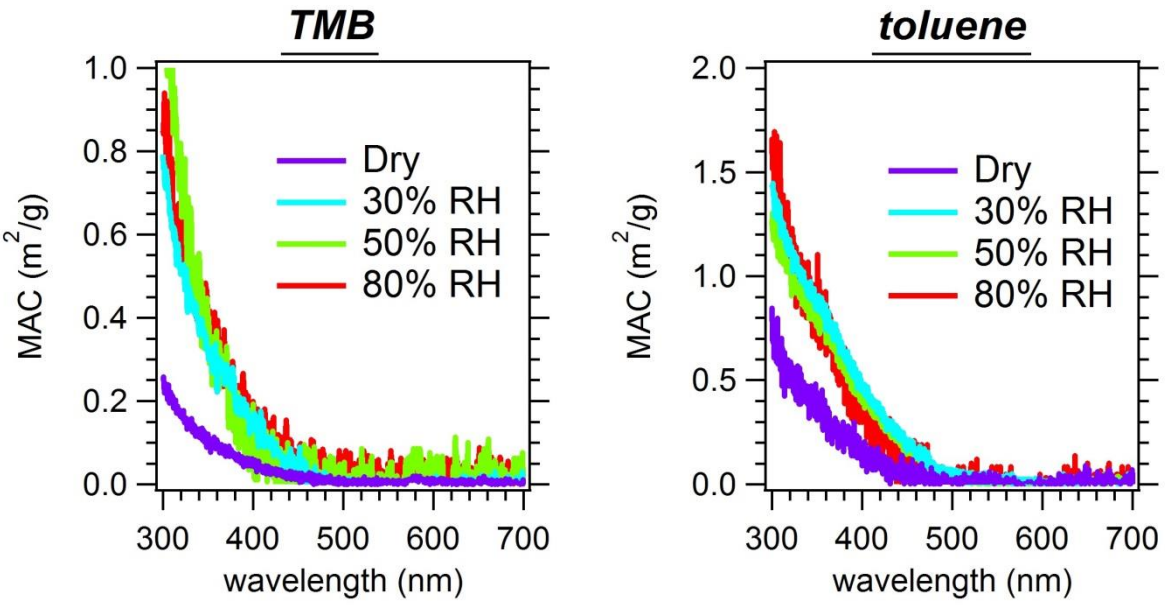

Figure 5. MAC spectra of TMB and toluene SOA formed at <5%, 30%, 50% and 80% RH.

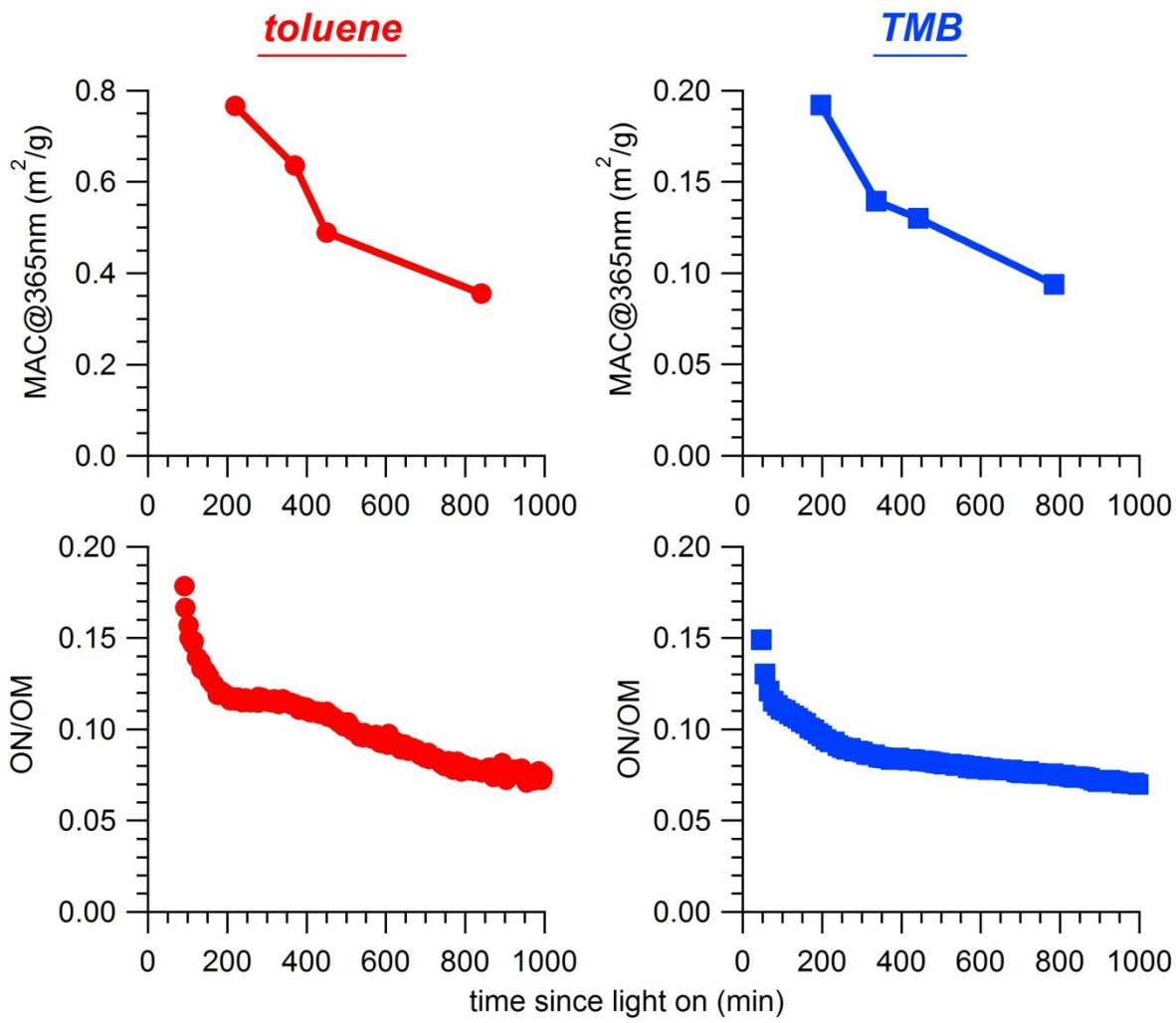

Figure 6.Measurements of the MAC values (at 365 nm) of toluene and TMB SOA formed at 30% RH in the presence of NO_x as a function of photochemical age (top panels). The bottom panels show the AMS-measured ON-to-OM ratio.

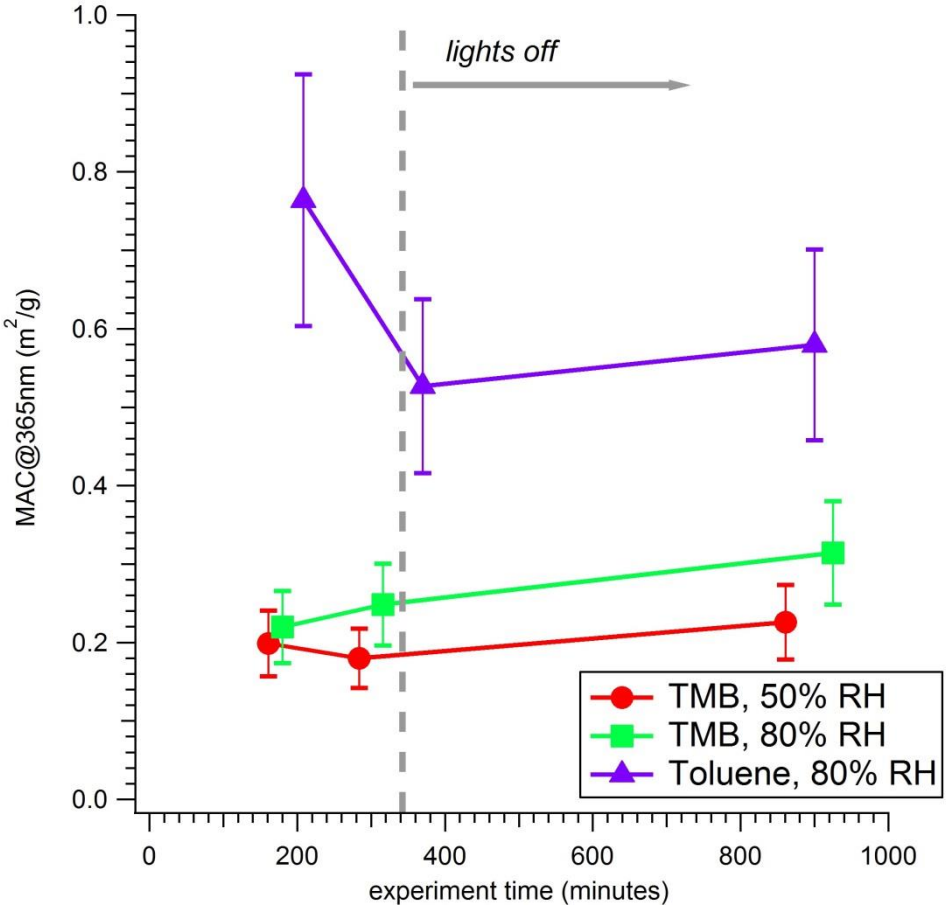

761

762 Figure 7. MAC values of aromatic SOA formed under high NO_x conditions and aged in the chamber
763 with the lights off at different RH levels.

764